

STRUCTURAL DESIGN OF MEDIUM SCALE COMPOSITE WIND TURBINE BLADE

C.D. Kong¹, J.H. Bang¹, J.C. Jeong¹, M.H. Kang¹, S.H. Jeong¹ and J.Y. Yoo²

¹ *Dept. of Aerospace Engineering, Chosun University, #375 Seosuk-dong,
Kwangju, Republic of Korea*

² *Hankuk Fiber Co., #181-1 Yongji-ri, BuBuk-myun, Miryang-si,
Kyungnam, Republic of Korea*

SUMMARY: In this study, the 750kW medium scale composite blade for the horizontal axis wind turbine systems was developed by using a specific structural design and test procedures. Loads acted on the wind turbine blade were firstly analyzed and compared to loads specified by the international specification IEC 1400-1. The blade designed was the box type, which was composed of the spar with the unidirectional Glass/Epoxy flange and the angle ply ($\pm 45^\circ$) Glass/Epoxy-urethane foam sandwich web for enduring bending and shear forces, and the fabric ($\pm 45^\circ$) Glass/Epoxy skin with the foam sandwich for enduring torsion and buckling. For the rotor hub, the insert bolt joint method was specially devised for reducing the weight of the blade. In the preliminary design phase, the Netting Rule based on the Principle Stress Design Method was applied to determine the size of the blade structure. And structural strength such as ply failure and buckling was preliminary investigated by the Classical Laminate Theory with Rule of Mixture. For linear static stress analysis, eigen value analysis and buckling analysis of the blade were analyzed by using FEM with the 3-D composite shell element. In the test, it was found that local buckling at the trailing edge of the blade and excessive deflections at the blade tip were happened. In order to solve these problems, the design of blade structure was modified. After improving the design, the abrupt change of deflection at the blade tip was reduced by smooth variation of the spar thickness and the local buckling was removed by extending the web length. The safety and stability of the blade structure of the modified design was reevaluated by FEM and structural test. And Fatigue life over 20 years was confirmed by using S-N linear damage method, Spera's method, etc.

KEYWORDS: composite wind turbine blade, fatigue life estimation, structural design, structural test

NOMENCLATURES

\vec{U}	Circumferential speed of the section at a distance r from the rotation axis
\vec{V}	Gust wind speed through the rotor
\vec{W}	The velocity of the airflow relative to the blade
β	Wind direction change
C_n	Normal force coefficient

C_t	Tangential force coefficient
ρ	Air density
l	Chord length
b_f	Width of flange
b_w	Height of web
A	Section area
X_t	Tensile strength
X_c	Compressive strength
E_x	Elastic modulus
\bar{E}_x	Equivalent elastic modulus
t_w	Thickness of web
N_x	Buckling load
K_0, C	Buckling constants depending on edge conditions, plate aspect ratio, etc.
D_{ij}	Flexural laminates stiffness
δM_y	Blade cyclic flat wise bending moment
δM_z	Blade cyclic chord wise bending moment
n	Number of standard derivations
a	Hub-rigidity factor
b	Tower-blockage factor
d	Air-density factor
e	Chord wise dynamic-amplification factor
f	Flat wise dynamic-amplification factor
g	Wind-variability factor
U_n	Wind speed at hub elevation

INTRODUCTION

There are two general types of wind turbine systems: such as the horizontal axis wind turbine (HAWT) and the vertical axis wind turbine (VAWT). The HAWT of these two types is predominantly used because of its good performance and high structural efficiency [1]. The rotor blade among the components of the wind turbine system transforms wind power to mechanical power. In general three blades are used for the wind turbine system to keep the dynamic balance and minimize the fatigue effect, and the blades are reduced weight by manufacturing with composite materials in order to secure structural strength and stiffness, fatigue life and low cost according to being large sized. Recently composite materials used in the blade of the wind turbine are E-glass/Epoxy, E-glass/Polyester, S-glass/resin, Kevlar/resin, Graphite or Carbon/Epoxy and Wood/Epoxy. Generally E-glass/resin is most widely used in the blade of the wind turbine because of its low cost and good performance [2]. Aerodynamic configuration for the blade is used from former NACA 4xxx series to recent NACA 65-xxx, NACA 63-xxx, etc. and is tapered from the root to the tip of the blade in general. Commonly used the structural configuration is a box type with shell-spar. And flange type, T-bolt type and insert bolt joint method are used to support heavy loads for the rotor hub joint part [3]. Although the design procedure of the blade is different each designing and manufacturing company, the common procedures are performing aerodynamic configuration design, dynamic and static load analyses, structural design, securing structural strength through static stress analysis, prediction of fatigue life from the random load spectrum and the modal analysis to prevent the resonance in order. In the structural load calculation, there were quasi-static aerodynamic load calculation, application of dynamic modeling method by A.D. Garrad

in 1983, development of a rotor blade using aero elastic tailoring by Shirk, *et al.* in 1986 and calculation using FEM by O.A. Bauchau. Recently the structural design procedures are developed, established and practically used by many companies such as VESTAS, Micon, Wind Energy Group, Enercon, Zond, Bonus, etc. [4][5].

In this study, the 750kW scale wind turbine blade was manufactured with E-glass/Epoxy which was produced in Korea and proved its properties, and used NACA 63-218 which has good starting characteristic and aerodynamic performance. The structural configuration was the box type using skin-spar-foam sandwich structure. And on the rotor hub joint part, the insert bolt joint method was used to reduce the weight of the blade. At the first design stage, after calculating a quasi-static ultimate load and an inertia load, structural dimensions which satisfied basic structural strength were determined, suitability to the design requirement was confirmed by analyzing deflections and twist angles with FEM, and the resonance was investigated by calculating the natural frequency and the mode of vibration through the modal analysis. From the results, the blade was manufactured and tested by the specific structural test rig. In the test, it was found that local buckling, delaminations and excessive deflections at the blade tip were happened. In order to solve these problems the design of the blade structure was modified.

DESIGN PROCEDURE AND RESULT OF AERODYNAMIC DESIGN

The design for the blade of the wind turbine is to determine the configuration, the structural type and materials of the blade that satisfy the design requirement including aerodynamic performance, structural strength and cost. Fig. 1 shows the design procedure for the blade of the wind turbine in this study. The rotor blade diameter, airfoil configuration, twist angle, tip speed ratio, etc. were obtained from wind conditions in the region in which the wind turbine system will be operated, and then the aerodynamic design was performed by using them. It was examined by the performance analysis program whether aerodynamic design results satisfied design requirement or not. From the aerodynamic configuration, the aerodynamic load according to various operating conditions was calculated and the structure design was performed in order to be operated safe keeping this load.

The reasonableness of the structural design results was examined by various analyses. The aerodynamic configuration was designed through determining the number of blade, airfoil configuration, thickness, chord length, variation of twist angle and rotor diameter which were obtained by applying rated rpm, rated wind speed, rated power, cut-in wind speed and maximum design wind speed by Betz, Strip and Vortex theories [6]. Table 1 shows the specification of the wind turbine system to design the aerodynamic configuration and Fig. 2 shows the result of the aerodynamic design.

Table 1 Specification of HAWTS

Rated Power	Cut-In Wind Speed	Rated Wind Speed	Cut-Out Wind Speed	Rotor Speed	Number of Blades	Blades Length	Airfoil
750kW	3.0m/s	12.5m/s	25m/s	15-35 RPM	3 Blades	23.3m	NACA 63-218

LOAD ANALYSIS

The structural design requirement was that the blade maintains the result of the aerodynamic design and keeps all actual loads with minimum weight.

Loads acted on the wind turbine system are divided into aerodynamic load and loads due to weight and motion of the blade, snow, centrifugal force in rotating, etc. [7]. It is difficult to analyze these loads because they are related to each other. Therefore, in this study the aerodynamic load mainly acted on the blade was analyzed.

In order to obtain the aerodynamic loads acted on the blade the main characteristics were considered the change of wind direction and the variation of the velocity due to the gust shown in Fig. 3. The velocity of the airflow relative to the blade at a distance r from the rotational axis was obtained by

$$W = \sqrt{U^2 + V^2 + 2UV \sin \beta} \quad (1)$$

The aerodynamic force which are acted on the blade section was calculated by

$$f_n = \frac{1}{2} \rho C_n l W^2 \quad , \quad f_t = \frac{1}{2} \rho C_t l W^2 \quad (2)$$

The aerodynamic force on the whole blade was obtained by integrating above forces from root to tip.

Wind speeds of 12.5m/s, 20m/s and 25m/s and the gust condition were considered. And on the stationary condition, the wind speed of 55m/s, which can be occurred once 190 years, was considered [8]. Table 2 shows the result of the analysis for wind speed of 20m/s. In order to confirm the validity of the load analysis method in this study, the result of the load analysis was compared to IEC1400-1, which is the international specification for the structural safety of WECS. Fig. 4 shows comparison between the load by this study and the load by IEC1400-1 at the rated wind speed of 12.5m/s.

Table 2 Results of load analysis for wind speed 20m/s

Station	F _N [kN] (Normal Force at Chord)	F _T [kN] (Tangential Force at Chord)	M _N [kNm] (Flapwise Bending Moment)	M _T [kNm] (Chordwise Bending Moment)
1.00	8.148	1.460	16.297	2.919
0.92	9.800	1.778	52.195	9.396
0.84	10.765	1.982	109.624	19.838
0.76	11.233	2.063	189.477	34.406
0.68	11.108	2.067	291.546	53.110
0.60	10.520	1.952	414.655	75.719
0.52	9.606	1.801	556.976	101.930
0.44	8.455	1.578	716.207	131.298
0.36	7.030	1.326	889.499	163.319
0.29	5.751	1.069	1074.296	197.478

PRELIMINARY DESIGN

Previously described various loads act on the rotor blade as types of bending, torsion and shear forces. Therefore, the basic structure of blade section was designed the box type as shown in Fig. 5. It was designed that the bending force was kept by the spar manufactured with unidirectional fiber, the torsion was kept by box type structure composed of the web and skin manufactured with the angle ply ($\pm 45^\circ$), and the shear force was kept by the web. Moreover in order to reduce the buckling due to the compression from the bending load, the foam sandwich structure was added on the inner skin of the leading and trailing edges. And the rear web was added near the trailing edge to prevent the buckling caused by twisting load. Table 3 shows the properties of materials used in this study.

Spar structure composed of flange and web was selected as basic structure of blade section and dimensions of flange and web was determined from aerodynamic configuration as the Table 4.

In order to determine the number of layers, strength analysis on unit ply laminate was carried out and the number of layers was determined on the basis of safety factor obtained from this strength analysis. Maximum aerodynamic load, which is gust condition of wind speed 20m/sec, was applied to laminate on preliminary design phase.

Table 3 Material properties

	Fabric	UD	Foam
Density [kg/m ³]	1750	1850	52.06
E _x [GPa]	24.8	31	0.07
E _y [GPa]	11	11	0.07
G [GPa]	4.14	4.14	0.019
Poisson's Ratio	0.27	0.27	0.2
F _{xc} [MPa]	174.6	620	0.896
F _{xt} [MPa]	313.7	777.8	1.896
F _{yc} [MPa]	138	138	0.896
F _{yt} [MPa]	31	31	1.896
F _s [GPa]	7.17	7.17	0.0008
Thickness [mm/ply]	0.445	0.49	12.5

Table 4 Dimension of blade section for preliminary design

Station	0.286R	0.356R	0.437R	0.517R	0.598R	0.678R	0.759R	0.839R
<i>b_f</i> [mm]	926	856	776	696	616	536	456	376
<i>b_w</i> [mm]	800	750	530	340	300	270	230	198

Structural design by Netting Rule is useful in preliminary design phase. In general, however, this design method induces weighted structure if Quasi-Isotropic Design Method is used in initial design phase. In this study, therefore, Principal Stress Design Method in which fiber was laminated along the direction of principal stress, was used to minimize the weight of blade.

Fig. 6 and 7 show stresses of spar flange and web respectively. Safety factor 5.0 was considered in preliminary design because the strength of E-glass Material decrease by 20% of

initial strength after required fatigue life, 20 years, from S-N curve shown in Fig. 8. Following stress condition was applied for the preliminary design.

$$\left| \frac{F_x}{A} + \frac{M_z(\pm y)}{I_z} \right| \leq \left| \frac{X_t}{5}, \frac{X_c}{5} \right| \quad (3)$$

In the same manner, web was designed by applying following condition.

$$\tau_{xy} = \frac{F_x}{A} \leq \tau_{xy}^* \quad (4)$$

Preliminary design results of spar flange and web are as shown in Table 5.

Table 5 Preliminary design result for spar flange and web

Station	0.286R	0.356R	0.437R	0.517R	0.598R	0.678R	0.759R	0.839R
Flange	(0°) ₁₄ s	(0°) ₁₄ s	(0°) ₁₅ s	(0°) ₁₆ s	(0°) ₁₅ s	(0°) ₁₃ s	(0°) ₁₂ s	(0°) ₁₀ s
	16.24t	16.24t	17.4t	18.56t	17.4	15.08t	13.92t	11.6t
Web	(+45°) ₁₀ s	(+45°) ₁₀ s	(+45°) ₁₁ s	(+45°) ₁₂ s	(+45°) ₁₁ s	(+45°) ₁₀ s	(+45°) ₉ s	(+45°) ₈ s
	12t	12t	13.2t	14.4t	13.2t	12t	10.8t	9.6t

Laminate strength analysis was performed by laminate analysis program using Classical Laminate Theory. Load intensities were calculated by using equivalent elastic modulus obtained from laminate sequence and material properties. And then S.F. was calculated by Maximum Strain Failure Criterion and laminate strength analysis using load intensities. Load intensities for unit length for each stress component of spar flange and web were obtained by following equations. (See Fig. 6 and 7)

$$N_{xf} = \sigma_{xf\text{total}} \cdot t_f$$

$$N_{xyf} = \frac{F_y}{I_z} \cdot t_f \cdot \frac{b_w}{2} \cdot \int_0^{\frac{b_w}{2}} ds \cdot \frac{E_{xf}}{E_x} = \frac{F_y}{I_z} \cdot t_f \cdot \frac{b_w}{2} \cdot \frac{b_f}{2} \cdot \frac{E_{xf}}{E_x} \quad (5)$$

$$N_{xw} = \sigma_{xw\text{total}} \cdot t_w$$

$$N_{xyw} = q_{xyw} = \frac{F_y Q}{I_z} \cdot \frac{E_{xw}}{E_x}, \quad Q = \int y dA = \int y t_w dS \quad (6)$$

Where, subscript *f* and *w* means flange and web respectively. Table 6 shows load intensities for unit length of spar flange and web

Table 6 Load intensities for spar flange and web

Station	0.286R	0.356R	0.437R	0.517R	0.598R	0.678R	0.759R	0.839R
N_{xf} [N/mm]	-1237.96	-1165.51	-1512.35	-2119.7	-2011.4	-1790.7	-1602.2	-1303.7
N_{xyf} [N/mm]	56.96	56.96	74.27	103.97	101.78	93.70	86.10	71.80
N_{xw} [N/mm]	-118.94	-111.98	-149.20	-213.84	-198.40	-185.30	-161.60	-140.30
N_{xyw} [N/mm]	116.29	116.33	151.10	210.15	206.00	189.80	174.30	145.70

Structural analysis results for laminates of preliminary design are shown in Table 7. According to analysis results, there were some undesirable design results, but the results were satisfied because simplified structure was considered in preliminary design. Table 8 shows bending stiffness derived from analysis and it is to be used in buckling analysis.

Table 7 Laminate analysis results

Station	S.F. (Spar Flange)		S.F. (Spar Web)	
	1 st Ply Failure	Last Ply Failure	1 st Ply Failure	Last Ply Failure
0.286R	6.24	15.74	4.64	14.16
0.356R	6.63	16.71	4.93	14.47
0.437R	5.48	13.80	4.07	12.13
0.517R	4.17	10.50	3.10	9.42
0.598R	4.12	10.38	3.06	9.00
0.678R	4.00	10.10	2.98	8.81
0.759R	4.14	10.42	3.07	8.78
0.839R	4.24	10.67	3.15	9.22

Table 8 Useful derived values for buckling analysis

Station	Spar Flange		Spar Web	
	$(D_{11} D_{22})^{0.5}$	$D_{12}+2 D_{66}$	$(D_{11} D_{22})^{0.5}$	$D_{12}+2 D_{66}$
0.286R	7.097E6	3.050E6	1.046E6	2.145E6
0.356R	7.097E6	3.050E6	1.046E6	2.145E6
0.437R	8.729E6	3.751E6	1.392E6	2.856E6
0.517R	1.059E6	4.553E6	1.807E6	3.707E6
0.598R	8.729E6	3.751E6	1.392E6	2.856E6
0.678R	5.682E6	2.442E6	1.046E6	2.145E6
0.759R	4.469E6	1.921E6	7.624E5	1.565E6
0.839R	2.586E6	1.112E6	5.354E5	1.098E6

Fig. 9 shows buckling load on spar flange. Critical buckling load was calculated by using bending stiffness and ESDU 80023 (see Fig. 10), and S.F. was calculated by comparing applying load and critical buckling load with following equation.

$$N_{xf} \leq N_{xcritical} = \frac{K_0(D_{11}D_{22})^{0.5}}{b^2} + \frac{C\pi^2(D_{12} + 2D_{66})}{b^2}, \quad b = \frac{b_f}{2} \quad (7)$$

Buckling reduction factors for spar flange are shown in Table 9.

Table 9 Buckling reduction factor for spar flange

Station	0.286R	0.356R	0.437R	0.517R	0.598R	0.678R	0.759R	0.839R
S.F.	1.47	1.83	2.11	2.27	2.52	2.43	2.95	3.09

Rotor Hub

Various methods to efficiently join the rotor blade made of composite materials to the rotor hub made of metal have been studied. Among them the flange bolt joint type and the T-bolt

joint type are mainly used in the HAWT [9][10]. In this study the insert bolt joint method that was specially devised for reducing the weight of the wind turbine and confirmed its safety through the parts test was used. (See Fig. 11)

Result of Stress Analysis by the FEM

The modeling of the designed blade was performed as shown in Fig. 12 and FEM analysis was performed in terms of applying previously obtained loads. The type of finite element used was the general 3-D composite shell element. Linear static stress analysis, eigen value analysis and buckling analysis of the spar on which mainly loads act were analyzed by using commercial FEM code, both NISA II and ANSYS. As a result, total weight of the blade was 2.63ton. For load distribution, stress concentration phenomena happened on the end of the spar and maximum stress of the skin was 63.5MPa at this point. By Tsai-wu failure criteria safety factor was above 3.5 and confirmed safe [11]. As a result of buckling analysis, buckling occurred at the trailing edge between 0.5r/R and 0.7r/R stations. But S.F. for buckling was above 10 and safe. Analysis results are shown in Table 10.

Table 10 Result of FEM analysis for first structural design

Weight [ton]	Max. Stress [MPa]			Max. Displacement [m]			Eigen Value [Hz]			
	Flap Mode		Lead-Lag Mode		Flap Mode		Lead-Lag Mode			
2.63	12.5	20	55	12.5	20	55	1 st	2 nd	1 st	2 nd
	[m/s]	[m/s]	[m/s]	[m/s]	[m/s]	[m/s]				
	39	63.5	127	1.089	1.685	3.318	2.25	8.24	2.32	5.47

MANUFACTURING AND STRUCTURAL TEST

The blade, which was divided into four parts, was manufactured. Upper and lower skins and front and rear webs were manufactured by the hand lay-up because there was not an available autoclave for the size of the structure. As stated above, the structure of the blade was too long to lay-up just once. Moreover there was a problem that the curing proceeded while resin was impregnated into glass fibers. However, the rotor hub which is a high stressed part was manufactured in the autoclave. Method to assemble the parts is as follows, the webs and the rotor hub were fixed to the lower surface and then the upper surface was put on and adhere to that, and the bonding area between upper and lower surface was extended by attaching patches to improve the bonding strength.

Manufactured blade is evaluated by comparing with design result through the structural test. Structural test procedure is shown in Fig. 13. In the test, applying load, strain and deflection were measured by using measurement system as shown in Table 11.

Table 11 Sensors and test equipment

Test Equipment	Use	
Strain Gage	Strain Measure	SEA-00-250UW-120
Load Cell	Load Measure	5 ton, 3ea used
Displacement Transducer	Displacement Measure	5ea used
SYS. 4000, AI 1600	Data Acquisition	40 Channel used

The manufactured blade was set on the test rig and loaded at 20.2m and 17.6m stations of the blade, and deformations and deflections of the blade were measured. AI1600 of CAS Co. was used as a measurement system and 4 displacement gages, 22 strain gages and a load cell were used in the test. Fig. 14 shows data acquisition system, AI 1600.

Load was applied according to the analysis result at the wind speed 20m/s including the gust condition. Test results were compared with FEM analysis results that obtained by applying load with an interval of 9.8kN. As a result of the comparison of the analytical values and the empirical values, generally both showed similar trend as shown in Table 12, but the analytical values were bigger than the empirical values by 10%. Load was acted as the concentrated load on 20.2m and 17.6m stations of the blade. In case of applying load on 20.2m station, debonding occurred between the upper and lower surface on load of 25.48kN, and therefore the test was interrupted. And in case of 17.6m station, local buckling occurred at the trailing edge of near 0.65r/R station under applying load of 49kN, and it was difficult to increase the load. Deflections of the blade were measured up to 1.74m at 41.16kN.

Table 12 Comparison between analysis and test results [First Prototype]

Tensile	Measuring Location [m]	3.0	6.0	10.0
	Analysis [MPa]	8.56	15.99	16.54
	Test [MPa]	3.21	15.20	22.01
Compressive	Measuring Location [m]	3.0	6.0	10.0
	Analysis [MPa]	-8.00	-15.23	-20.08
	Test [MPa]	-7.98	-13.80	-18.77

The major problems found in the structural test were as follows. Firstly, the weight of the manufactured blade was 3.2ton and was heavier than the design weight by 0.4ton. This was caused by attaching patches to improve the strength through increasing the bonding area to joint upper and lower skins of the blade. Secondly, there was abruptly excessive deflections caused by the concentrated stress on the end of the spar. Such the excessive deflections must be considered on the design modification because it will affect the aerodynamic performance. Finally, local buckling happened at the trailing edge near 0.65r/R station of the blade.

DESIGN MODIFICATION

Design Modification

The design of the blade was modified to solve excessive deflections and local buckling of previously described problems. In order to diminish the stress concentration on the spar, abrupt variations of thickness of the spar were reduced. One UD ply was added to the leading edge of the blade and the rear web was extended to 0.678r/R station so that local buckling would not happen. Fig. 15 and 16 show the sectional configuration and the lay-up stacking sequence of the modified blade design respectively.

Structural Analysis for Modified Design

As a result of structural analysis, total weight of the blade was reduced by 0.3ton. However the stress was slightly increased on the whole structure, but the stress concentration

region was removed, maximum stress region was moved into 0.286r/R station and acted on the spar of this station. Though the stress was slightly increased in the previous design the maximum stress was found on the skin but in the modified design it was found on the spar, so that it was confirmed that structure was safer as the factor of safety was above 9. Deflections increased by 10% compared with the former design but the type of deflections was changed from an abrupt type affected the aerodynamic performance into smooth deflections type. The result showed that the modified design was more effective.

In the result of buckling analysis for the spar, buckling was found at 0.286r/R station of the blade and the factor of safety was above 3, and in the result of buckling analysis for the trailing edge the factor of safety was above 2 so that the safety for buckling was confirmed. As a result of the natural frequency analysis, the natural frequency of the modified design was lower by 15% than that of the former design and the resonance in operating was not found as shown in Fig. 17. Fig. 18 and Table 13 show the results of the structural analysis.

Table 13 Result of FEM analysis for modified design

Weight [ton]	Max. Stress [MPa]			Max. Displacement [m]			Eigen Value [Hz]			
							Flap Mode		Lead-Lag Mode	
	12.5 [m/s]	20 [m/s]	55 [m/s]	12.5 [m/s]	20 [m/s]	55 [m/s]	1 st	2 nd	1 st	2 nd
2.36	44.9	72.2	144	1.2	1.834	3.387	1.89	5.43	2.33	7.5

Fatigue Life Estimation

In this study, the required fatigue life which must be safely operated more than 20 years and should be met by the International Wind Turbine Safety Regulation IEC1400 Part I, was estimated.

The fatigue allowable stress was calculated by the following S-N linear damage equation [1],

$$S_{\max \max} = S_I \left[N_f \frac{\sum_{i=1}^n n_i R_i^{13.5}}{\sum_{i=1}^n n_i} \right]^{-0.074} \quad (8)$$

where, S_I is the empirical stress coefficient by Mandell's empirical equation, R_i is the stress ratio for the i_{th} layer which was obtained from the load spectrum in the field test of the similar wind turbine blade, and N_f is the required 20-year design life cycles. Table 14 shows the result of the calculation for the required life, where the knock-down factor was considered to account for scatter in the laboratory test data and several condition that can be reduce in full-scale structures below that of laboratory specimens.

Table 14 The result of fatigue stress calculation

N_f [cycle]	S_I [MPa]	$S_{\max \max}$ [MPa]	$S_{\max \max} \times (\text{KDF})$ [MPa]
3.72×10^8	363.63	101.2	80.96

In order to obtain the cycle loads, the following empirical equations, which were proposed by D.A. Spera, were used in this study [13][14].

$$\delta M_{y,n} = aM_g \sin \theta + 432(1 + 1.47a) \times cd(g + 0.012b) \times U_n(1-s) \exp^{(0.134n)} (D/100)^4 \quad (9)$$

$$\delta M_{z,n} = eM_g + 46.8cd(g + 0.1b) \times U_n(1-s) \exp^{(0.276n)} (D/100)^3$$

Table 15 shows the result of the calculation for the 750kW class wind turbine blade. The maximum compressive stress for these cyclic loads, which was analyzed by FEM, was 52.84MPa. Because this cyclic maximum stress in operation is less than the required fatigue allowable stress 80.96MPa, the required fatigue life for the 750kW class wind turbine blade would be confirmed to be met over the required 20-year design life.

Table 15 The result of fatigue load calculation [kN.m]

n	$\delta M_{y,cyc}$	$\delta M_{y,max}$	$\delta M_{z,cyc}$	$\delta M_{z,max}$
0	67.9	215.5	226	265.3
1	105.6	335.2	232.1	272.5
2	165.1	524	243	285.3

Structural test for design modification

In order to prevent excessive deflection and stress concentration found in the first prototype blade test, aerodynamic load with gust condition at wind speed 20m/sec was applied to three points of the second prototype blade in the test. Table 16 shows each load point and load size determined from moment diagram as shown in Fig. 19 and load was applied by test rig manufactured as shown in Fig. 20 and 21.

Table 16 Load value and loading point for structural test [Second Prototype]

Loading Position	17.1m	20.26m	21.85m
Load Size	3.5tonf	3tonf	2tonf
Measuring Range	6m ~ 16m		

Table 17 shows the test results for the second prototype designed to solve problems found at the first prototype test results. As a result of comparison between test and design result, it was found that there are differences of 30% in compression and 10% in tension. It is understood that the differences were induced by incomplete cohesive of inter lamina.

Table 17 Comparison of test and analysis results [Second Prototype]

Tensile	Measuring Location [m]	2.97	5.84	11.64
	Analysis [MPa]	15.89	20.62	17.71
	Test [MPa]	17.16	20.82	18.59
Compressive	Measuring Location [m]	9.92	13.6	15.61
	Analysis [MPa]	-25.92	-9.07	-20.97
	Test [MPa]	-33.95	1-1.15	-25.79

CONCLUSION

In this study, the 750kW scale composite blade for the wind turbine system was designed and manufactured, and it was tested and evaluated by the specific structural test rig. In order to solve the problems found in the test the design of the blade was modified.

As a result of modifying the design, total weight of the blade was reduced, the concentrated stress was removed by changing lay-up stacking sequence and thickness of the spar, so that the safety of the blade was high, abrupt deflections at the blade tip was reduced by smooth variation of the spar thickness to improve the aerodynamic performance and efficiency, and local buckling of the trailing edge was removed by extending the web length. And the safety for the joint part of the blade and the rotor hub was secured by using the shear pins. The required fatigue strength was calculated by S-N linear damage method. Fatigue load was obtained by using load spectrum through experiments and Spera's method. Service fatigue stress was analyzed by FEM with the calculated fatigue load. From comparison of the fatigue stresses with the required fatigue strength, the 20-year fatigue life was confirmed.

REFERENCES

1. Spera D.A., Wind Turbine Technology, *ASME Press*, 1994
2. Dieter G.E., Assessment of research needs for wind turbine rotor materials technology, *National academy press*, 1991
3. Garad A.D., Dynamics of wind turbine, *IEEE*, 1983, 130
4. Snel H., Program for HAWT analysis and simulation, *12th ASME Wind Energy Symposium*
5. Wright A.D., The use of ADAMS to model the AWT-26 prototype, 1994
6. Gourieres, Wind Power Plants, *Pergamon Press*, 1982
7. Eggleston D.M., Wind Turbine Engineering Design, 1987
8. Thom H.C.S., New distributions of extreme winds in the united states, *ASCE structural division*, No. 6038.
9. Tsai S.W. and Hahn H.T., Failure analysis of composite materials, inelastic behavior of composite materials, *ASME New York*, 1975, : 73-1975.
10. Hald H. and Kensche, Development and test of a light weight GRP rotor blade, *Proceedings Wind Power '85*, 1985
11. Mayer R.M. Design of Composite Structures Against Fatigue, 1996
12. Kong C.D., et al., Study on Aerodynamic and Structural Design of Large Scale HAWT Composite Blade, *3rd year-Final Report*, 1999
13. Spera D.A., Dynamic Loads in Horizontal-Axis Wind Turbines Part II : Empirical Equations, *Windpower '93*, 1993
14. Kong C.D., et al., Aerodynamic and Structural Design for Medium Size Horizontal Axis Wind Turbine Rotor Blade with Composite Material, *KSPE*, 1997, 1, (2): 12-21.

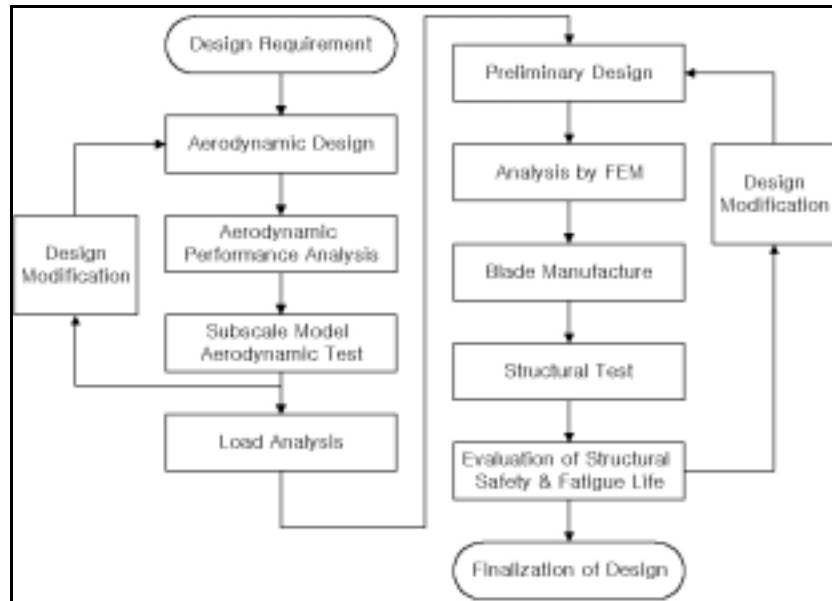


Fig. 1 Flow chart for blade design

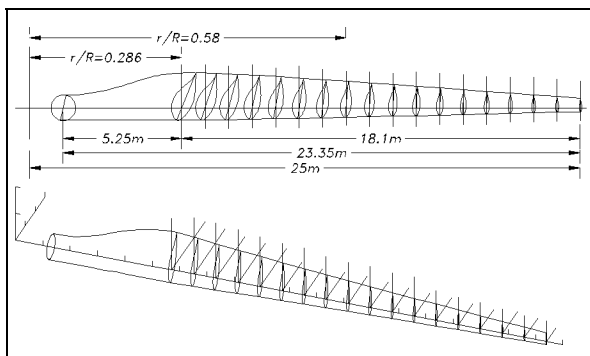


Fig. 2 Result of aerodynamic design

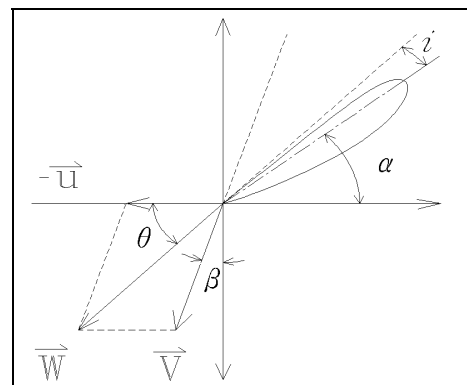
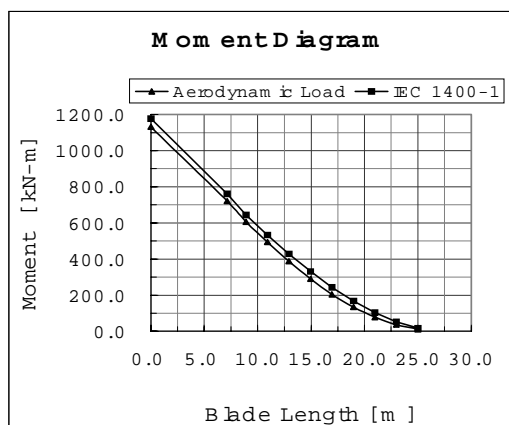


Fig. 3 Flow velocity



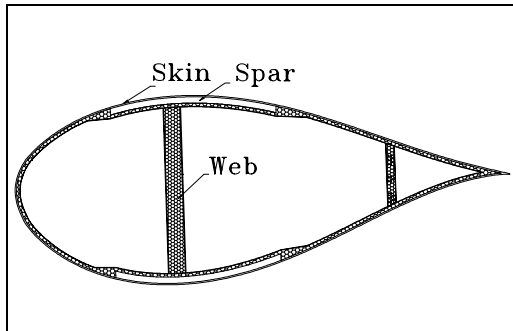


Fig. 4 Moment diagram at rated wind speed

Fig.5 Sectional Configuration

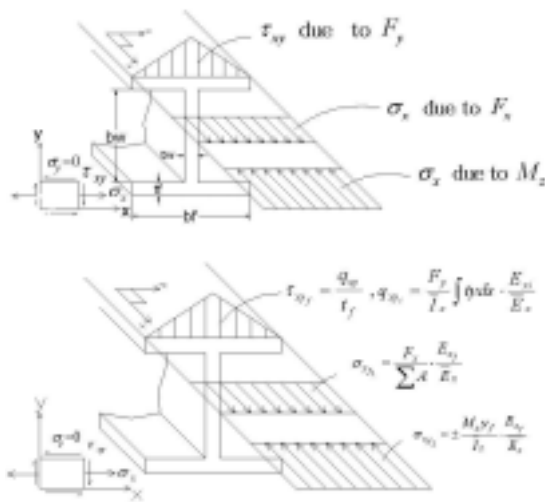


Fig. 6 Acting stress for spar flange

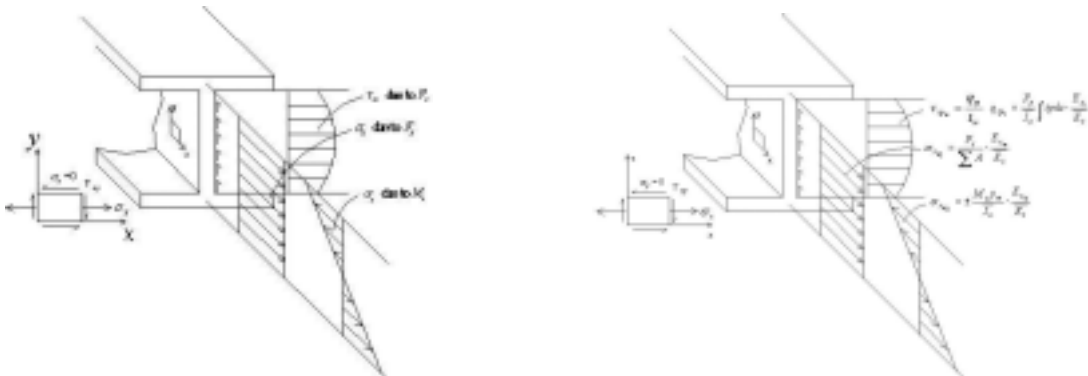


Fig. 7 Acting stress for spar web

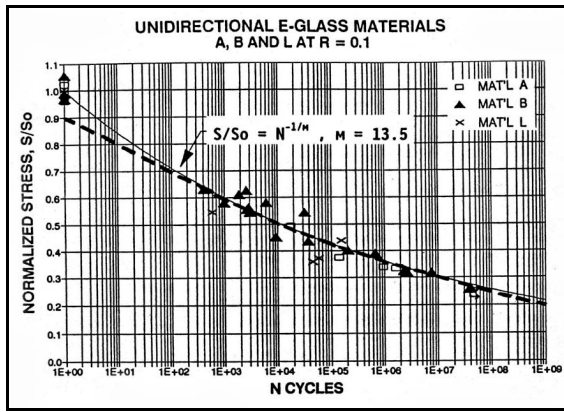


Fig. 8 S-N curve for UD E-glass material

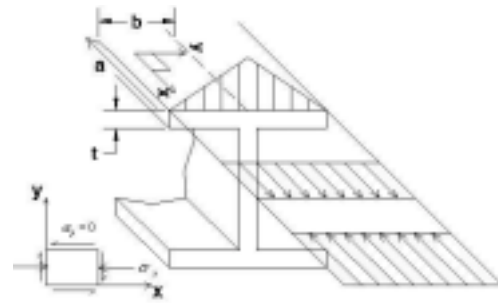


Fig. 9 Buckling load for spar flange

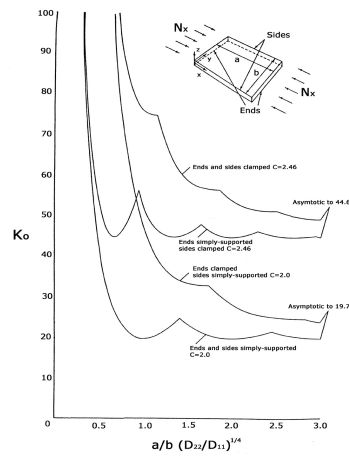


Fig. 10 ESDU 80023

